Comparison of Quantum Dots and CM-DiI for Labeling Porcine Autologous Bone Marrow Mononuclear Progenitor Cells

Michael Rutten*, Michael Ann Janes, Bryan Laraway, Cynthia Gregory and Kenton Gregory

Oregon Medical Laser Center/Oregon Center for Regenerative Medicine, Providence St. Vincent Medical Center, Portland, OR 97225, USA

Abstract: Autologous bone marrow mononuclear progenitor cells (ABMCs) are now being used for several regenerative medicine studies, but questions remain on the fate and function of the injected ABMCs. The ability to track the cells within animals is important in understanding the regeneration process, and both quantum dots (Q-dots) and the organic dye CM-DiI have been used frequently in cell tracking studies. Since there has not been a comparative analysis of Q-dots and CM-DiI for labeling ABMCs, the aim of the following study was to examine these probes for their ability to label ABMCs and to determine if the labeling affected the ABMC function. We found that ABMCs were easily labeled with either Q-dots or CM-DiI, with the CM-DiI being faster to load within the cells. Both Q-dots and CM-DiI could still be detected in the ABMCs after 10 days in culture. The loading of the ABMCs with CM-DiI had no effect of the ABMCs to form colonies in a CFU-F assay or on cell proliferation over two weeks. The labeling of the ABMCs with Q-dots had a small but significant inhibitory effect on CFU-F formation as well as inhibition of cell proliferation at two weeks. There was no effect of Q-dots on cell viability immediately after labeling. In summary, both Q-dots and CM-DiI can be used to label ABMCs, but CM-DiI was found to be more advantageous due to its faster loading time, ease of use, and lack of effect on colony formation and proliferation.

Keywords: Autologous bone marrow, Quantum dots, CM-DiI, cell labeling, CFU-F, proliferation, regenerative medicine.

INTRODUCTION

Cell transplantation using adult bone marrow mononuclear progenitor cells (ABMCs) is currently being investigated as a potential therapy to treat a wide variety of injured tissues. In animal studies it has been demonstrated that ABMCs contribute to the repair of injured hearts [1-4], kidneys [5, 6], livers [7], spinal cords [8], and peripheral nerves [9-11]. It has also been shown in a mouse model of myocardial ischemia that ABMCs exhibited a more favorable survival pattern as compared to the use of mesenchymal stem cells, skeletal myoblasts, and fibroblasts [12]. The use of ABMCs for clinical trials has also been reported in the treatment of damaged hearts [13-17] and peripheral arterial disease [18-22]. Although it has been demonstrated that the use of ABMCs can facilitate the restoration of some tissue function or repair, it is still not completely understood how this process takes place [23, 24]. Possible mechanisms include suppression of the local inflammatory response [25], secretion of local paracrine factors [26], or the possible ABMC transdifferentiation into the local host cell type [27]. One potential approach to resolving these issues is to be able to label and track ABMCs in a preclinical model to determine the specific fate of the injected cells.

Several different methods and probes have been used for labeling and tracking stem cells including 2-[18F]-fluoro-2-deoxy-D-glucose [28], magnetic resonance imaging, positron emission tomography, single-photon emission computed tomography [2, 29-31], as well as reporter gene analysis [32]. However, many of these methods are expensive to use and require special equipment for use in large animal preclinical studies. Other cell labeling probes that have shown to be effective in labeling stem cells as well as finding the cells in histological samples have been the organic fluorescent dye CM-DiI [33, 34] and fluorescent Quantum dot (Q-dot) nanocrystals [35, 36]. CM-DiI can also be rapidly loaded into cells facilitating its use with fragile cells. When CM-DiI was used to label mesenchymal stem cells, they could be detected in fixed heart tissue at two months [37], in skeletal tissue at six weeks [33], and heart tissue at 6 months [38] after injection. CM-DiI labeling is also retained when using conventional fixatives, whereas some fixatives can alter the detection of Q-dots within cells [39]. Q-dots do have several advantages over the use of organic dyes for labeling and tracking cells including their variety of sizes, emission wavelengths, high fluorescent quantum yield, and photostability for imaging [40-42]. However, the retention of Q-dots within stem cells can vary widely depending upon cell type or the Q-dot size used. For example, the 655 nm Q-dots were essentially lost from a culture of labeled murine embryonic stem cells (<1% positive cells) after 1 week of culture [43], while they were still detectable in a culture of labeled human mesenchymal stem cells after 8 weeks of culture [44]. Using human mesenchymal stem cells it was also found that after four days of labeling that ~85% of the 605 nm Q-dots was retained in the cells but there was little retention of 525 nm Q-dot [45].

*Address correspondence to this author at the Oregon Medical Laser Center/Oregon Center for Regenerative Medicine, 9555 SW Barnes Rd., Suite 210, Portland, OR, 97225, USA; Tel: (503) 216-2269; Fax: (503) 216-5256; E-mail: michael.rutten@providence.org

1876-8938/10

Although CM-DiI and Q-dots have been used successfully to label certain types of stem cells, there has not been a study comparing CM-DiI and the full series of Q-dots (Q-trackers) for labeling autologous adult bone marrow mononuclear progenitor cells. The aims of the current study were to examine the ability of CM-DiI and Q-dots to label adequately adult ABMCs, and to determine what effects these probes may have on cell function.

MATERIALS AND METHODS

Bone Marrow Collection and Mononuclear Cell Purification

All bone marrow samples were collected from 3-4 month male and female domestic swine (Swine Center, Washington State University, WA). The procedures of handling and care of the animals were strictly performed in accordance with the 2004 National Research Council "Guide for the Care and Use of Laboratory Animals" and following protocol approval by the Institutional Animal Care and Use Committee (IACUC) of the Legacy Clinical Research and Technology Center, Legacy Health System, Portland, OR. Under local anesthesia, 37 mls of porcine bone marrow was aspirated from each donor's iliac crest into a syringe containing 5 mls of heparin (1000 USP units/ml). The bone marrow was then transferred into a 150 ml transfer bag (Baxter, Deerfield, IL) containing 8 mls of citrate-phosphate dextran (Sigma, St. Louis, MO). The bone marrow transfer bag was then connected to a CS-900 cartridge kit (CS-900, Biosafe America, Houston, TX). This cartridge contains a wash-buffer bag that was filled with Hanks' balanced salt solution with cations (HBSS) (Invitrogen), a density gradient solution/waste bag that was filled with 100 ml of Histopaque®-1077 (Sigma, St. Louis, MO), and a third 150-ml transfer bag (Baxter, Deerfield, IL) used to recover the purified bone marrow. The bone marrow cells were then processed using an automated, completely enclosed cell processing device (SEPAX, Biosafe America) [46]. The final purified bone marrow mononuclear progenitor cell (BMC) product was collected in HBSS, and the ABMCs were counted with a Beckman Z2-Coulter Counter (Brea, CA).

Cell Labeling

CM-DiI Cell Labeling

The cell tracker CM-DiI (*Chloromethylbenzamido-1,1'-Dioctadecyl- 3,3,3'3'- Tetramethylindocarbocyanine Perchlorate*; Molecular Probes, Eugene, OR) stock solution was prepared using a modification of the manufacturer's instructions. From a 1 mg/ml CM-DiI stock solution in culture grade DMSO (Sigma, St. Louis, MO), 4 μM and 8 μM solutions were made in 500 μl of HBSS, vortexed, and then combined with 2 x 10^7 SEPAX purified ABMCs in 500 μl of HBSS to give final concentrations of 1 x10^7 cells/ml in either 2 μM and 4 μM CM-DiI labeling solutions. The CM-DiI cell suspensions were incubated for 15 minutes at 37°C, after which the cells were centrifuge at 800 x *g* for 40 seconds, washed once with 500 μl of HBSS at 800 x *g* for 40 seconds, then the pellet resuspended in 1 ml of α-DMEM media (Invitrogen, Carlsbad, CA). Since the stock CM-DiI was dissolved in DMSO, the final loading concentrations of CM-DiI at 2 μM and 4 μM represent DMSO concentrations of 0.2% and 0.4%, respectively, which were also tested as solvent controls. The labeled CM-DiI cells were then suspended in α-DMEM and plated into 35 mm glass dishes, 8-multiwell glass chambered slides, or 96-multiwell plates for growth studies. Both CM-DiI labeled and unlabeled cells were used for cell growth studies with cell numbers determined using a Coulter counter. For imaging studies, the cells were visualized using a Zeiss LSM 510 Meta confocal microscope (Zeiss, Thornwood, NY) using excitation/emission wavelengths of 553nm/570nm respectively.

Q-Dot Cell Labeling

The Q-trackers 525, 565, 585, 605, 625, 655, 705, and 800 nm cell labeling kits (Molecular Probes, Eugene, OR) were used according to the manufacturer's instructions. A 10 nM Q-dot loading solution were prepared by premixing 1μl each of Q-tracker Component-A and Component-B in a 1.5 ml microcentrifuge tube for 10 minutes at room temperature. Next 0.2 mls of α-DMEM media (Invitrogen, Carlsbad, CA) was added to each tube, the tubes were vortexed for 30 seconds, then 1 x 10^7 cells in 800 μl of α-DMEM were added to each tube. The tubes containing the cells and Q-dots were vortexed and then incubated at 37ºC for 60 minutes. The labeled cells were then washed and centrifuged at 800 x *g*, resuspended in α-DMEM medium and then plated into either 35 mm glass dishes, 8-multiwell glass chambered slides, or 96-multiwell plates for growth studies. For imaging studies, the Q-dot loaded cells were visualized with a Zeiss LSM 510 confocal microscope while excited with light at the appropriate excitation wavelength for each color of Q-dot nanocrystals.

Cell Culture

For cell proliferation and imaging studies, the labeled ABMCs were plated into 96-multiwell plates (Fisher Sci., Pittsburg, PA) or 35 mm glass dishes (Bioscience Tools, San Diego, CA), respectively. The cells were plated in α-DMEM (Invitrogen) supplemented with antibiotics and 10% serum (Invitrogen, Carlsbad, CA)). For all cell culture studies the media was removed and replaced every other day. For imaging studies the CM-DiI labeled cells were fixed with 5% Zinc-formalin for 10 min, counterstained with DAPI (Molecular Probes, Eugene, OR) for 1 min, then Cytoseal (Fisher Sci., Pittsburg, PA) anti-quenching mounting medium added. The Q-dot labeled cultures were fixed with 2.5% paraformaldehyde for 10 min, counterstained with DAPI for 1 min, and then Prolong Gold (Molecular Probes, Eugene, OR) added as an anti-quenching agent.

Colony Forming Unit-Fibroblast Assays (CFU-F)

SEPAX-purified ABMCs were suspended in Complete Mesencult media (Stem Cell Technologies, Vancouver, BC, Canada), and plated in T-25 flasks at concentrations of 0.5, 1.0, and 2.0 x 10^6 cells/ml in 5 ml of medium. The cells were cultured for 7 days in a 37°C humidified 5% CO_2 incubator (Thermo-Fisher Sci., Pittsburg, CA). To assess colony formation the media was removed, the flasks were washed twice with HBSS and then 5 mls of methanol (99.9%, Sigma, St. Louis, MO) was added to each flask for 5 minutes at room temperature to fix the cells. The methanol was then removed and the flasks were washed once with HBSS. After

allowing the flasks to air dry overnight at room temperature, 5 ml of 1 mg/ml Giemsa Staining Solution (EMD Chemicals) in methanol was added to each flask and again the flasks were incubated overnight, though at 4ºC. The next day the Giemsa stain was removed, the flasks were rinsed several times with HBSS, allowed to air dry at room temperature, and then the colonies were counted using an electronic colony counter (Bel-Art, Fisher Sci., Pittsburg, PA). A linear relationship between the plated cell numbers and the resulting colony forming unit numbers was within approximately 10-40 colonies per T-25 flask.

Cell Proliferation Assays

ABMC proliferation was measured using the MTT proliferation/cytotoxicity assay (Sigma, St. Louis, MO) according to the manufacturer's instructions with some modifications as follows. ABMCs, either unlabeled or labeled with 4 μM CM-DiI or 20 nM Q-dots, were plated at 1 x 10^4 cells/well in a 96-multiwell plate and cell growth measured at 7, 10, and 14 days. At 7, 10, and 14 days, 20 μl of a 5 mg/ml MTT solution in HBSS was added to each well of the multiwell plate. The multiwell plate was then incubated in a 37°C humidified 5% CO_2 incubator for 4 hours to allow the MTT to be metabolized. At the end of this time, 100 μl of an isopropanol/0.4N HCl solution (150:1 isopropanol:HCl using 6N HCl) was added to each well and the contents pipetted repeatedly to mix the solutions so that the metabolized formazan crystal products dissolved. The multiwell plate was then read on a Tecan microplate reader at an optical density (OD) of 570 nm with a background subtraction at 630 nm. The results of the CM-DiI and Q-dot-labeled BMC proliferative results were normalized to the control unlabeled cells and plotted over time as the Proliferation Index where a value of 1.0 represented no difference in the OD of the labeled to the unlabeled cells.

Live-Dead Assay for Q-dot Cytotoxicity

ABMC viability was tested using modified instructions from a commercially available kit (Live-Dead Viability Assay Kit, L-3224, Molecular Probes, Eugene, OR). The Live-Dead assay probe solution consisted of 5 μl of the supplied 2 mM EthD-1 stock solution and 2.5 μl of 4 mM calcein-AM stock solution to 5 ml of Hanks solution. The Hank's dye mixture was vortexed then added to unlabeled and Q-dot labeled ABMC that were plated for one hour in an 8-multiwell chambered glass slide. Because of the potential inference of the Q-dot emission wavelengths with the calcein-AM or ethidium bromide in this assay, only the 655 nm Q-dots could be used for this part of the study. After 30 minutes the stained ABMCs were photographed by a Zeiss 510 confocal microscope to determine the percentage of live and dead cells using a 488nm excitation wavelength for calcein-AM and 514nm excitation wavelength for the EthD-1 to determine the number of dead cells. Photographs were taken by the confocal microscope then converted into JPG files and imported into NIH ImageJ. The photographs are then split into red and green images and the number of cells counted in each image and put into a table. The percentage of live cells was determined by the ratio of the overall number of live cells (green cell staining) to the total number of live and dead cells (green and red cell staining).

Imaging and Analysis

Imaging of cultured cells was done using a Zeiss 510 Meta confocal laser scanning microscope with a Chameleon laser system (Coherent, Santa Clara, CA). All images were taken with either an EC-Plan NeoFluar 40X (NA 1.3) oil immersion or a Plan-APOCHROMAT 63X (NA 1.4) oil-immersion lens. In some cases serial Z-stack images were made of the cultured cells with step size ranging from 0.5 to 1.0 μm and the images collected and reconstructed using Zeiss image analysis software. To quantify the relative Q-dot BMC labeling efficiency, a series of images were analyzed using a fluorescence emission profile for each Q-dot color and compared to DAPI stained cells within a 4-11 μM diameter range [47]. To quantify the relative BMC CM-DiI labeling efficiency, the numbers of CM-DiI and DAPI-stained cells were counted from image files analyzed using NIH Image-J software and the watershed application to prevent cell count overlapping.

Statistical Analysis

In order to compare CM-DiI and Q-dot labeled ABMCs with unlabeled cells, statistical comparisons were done using a one-way repeated measure analysis of variance (ANOVA) to test for significant differences between labeled and unlabeled cell groups. If differences between groups were detected then multiple comparisons versus control were done using the Holm-Sidak test for pair wise comparisons. In some cases if just two groups were compared (unlabeled vs. labeled) then a paired *t*-test was done. All statistical analyses were performed with Sigma Stat software (Systat Software, San Jose, CA), and statistical significance determined at a value of $p < 0.05$ with the results being presented as mean ± SEM.

RESULTS

Optimization of Q-dot and CM-DiI Loading into Bone Marrow Cells

We used a wide spectral series of Q-dots (525, 565, 585, 605, 625, 655, 705, and 800 nm) to assess the ability of Q-dots to label SEPAX-purified ABMCs. The labeling efficiency for each of the Q-dot sizes was assessed from Z-stack confocal images of ABMCs fixed and counterstained with DAPI 4 hours after they were loaded with Q-dots. When the ABMCs were loaded with a 10 nM concentration of Q-dots for 1 hour as outlined in the manufacturer's instructions, we found that the ABMCs were not equally labeled by the various sizes of Q-dots. Specifically, there were very few to no 525 nm or 565 nm Q-dots in the ABMCs compared to strong BMC labeling by Q-dots $\geq$ 585 nm (Fig. **1**). The low presence of 525 nm and 565 nm Q-dots was not a function of the 458 nm excitation laser line since similar results were seen at other excitation wavelengths of 425, 477, and 488 nm. However, when the Q-dot loading procedure was adjusted to increase both the Q-dot and coating peptide concentrations two-fold to 20 nM, we found that ABMCs were readily labeled by the 525 nm and 565 nm Q-dots (Fig. **2**). Although the individual number of Q-dots per cell was found to vary within the BMC population, we found that 89 ± 6% (n = 8) of the ABMCs contained one or more Q-dots within the cytoplasm when analyzed by cross

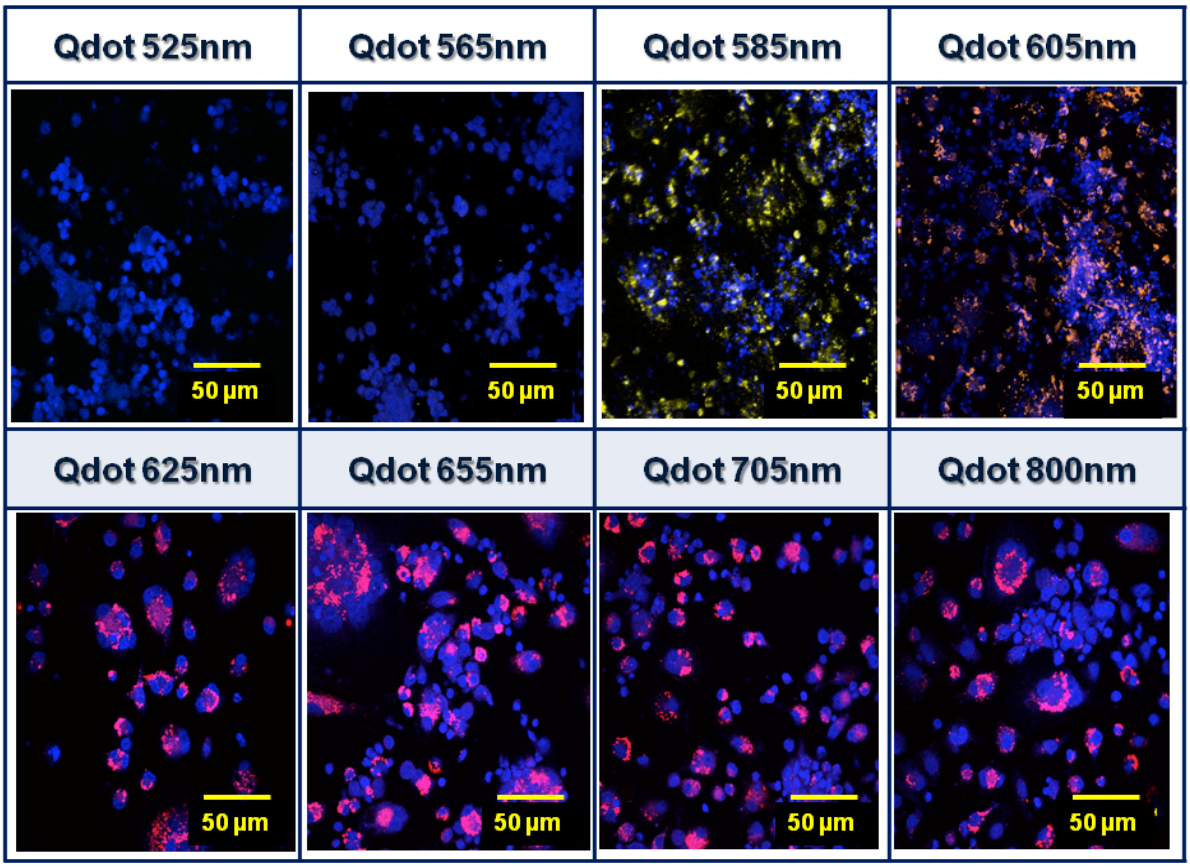

Fig. (1). Q-dot markers of different sizes do not label porcine ABMCs equivalently. ABMCs were loaded with 10 nM labeling solutions of Q-dots and 4 hours later labeling was assessed by confocal microscopy. Note that the 525 nm and 565 nm Q-dots loaded poorly into the ABMCs whereas larger Q-dots (>585 nm) all successfully loaded into the bone-marrow cells. The nuclei (blue) were stained with DAPI.

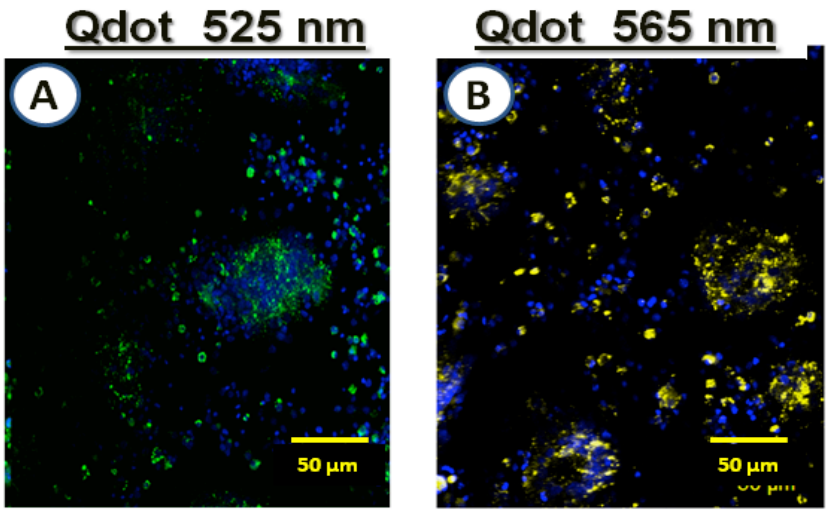

Fig. (2). Porcine ABMCs can be labeled with 20 mM solutions of 525 and 565 nm Q-dots. Representative confocal photographs of 525 nm (**A**) and 565 nm (**B**) Q-dot-loaded pig ABMCs. The loading solutions were twice that of those used in Fig. (**1**). The nuclei (blue) were stained with DAPI.

sectional Z-stack fluorescence emission (Fig. **3**). When the Q-dot loaded ABMCs were placed into culture for 10-days we found that 76 ± 2% of the cells (n =6) retained the Q-dot label (Fig. **4**).

CM-DiI labeling of ABMCs was assessed using 2 µM and 4 µM CM-DiI labeling solutions as we found CM-DiI concentrations $\geq$ 6 µM to have toxic effects on the ABMCs (data not shown). We found that uniform staining of the

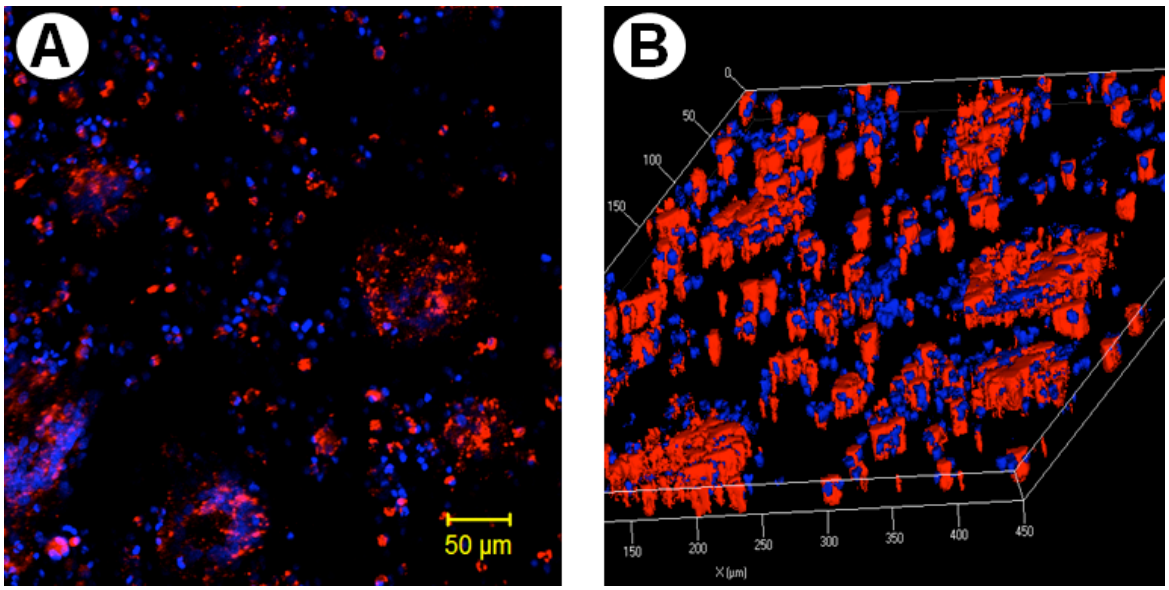

Fig. (3). Q-dots load into the majority of porcine ABMCs. While the number of Q-dots/cell varied, 82 ± 6% of ABMCs contained some Q-dots (n = 8). (**A**) A representative confocal photograph of 625 nm Q-dot labeled ABMCs at 4-hrs after labeling showing the distribution of Q-dots in the cells. (**B**) Three dimensional reconstruction of Z-stack imaged cells showing the overall localization of the Q-dots within the cells. The nuclei (blue) were stained with DAPI.

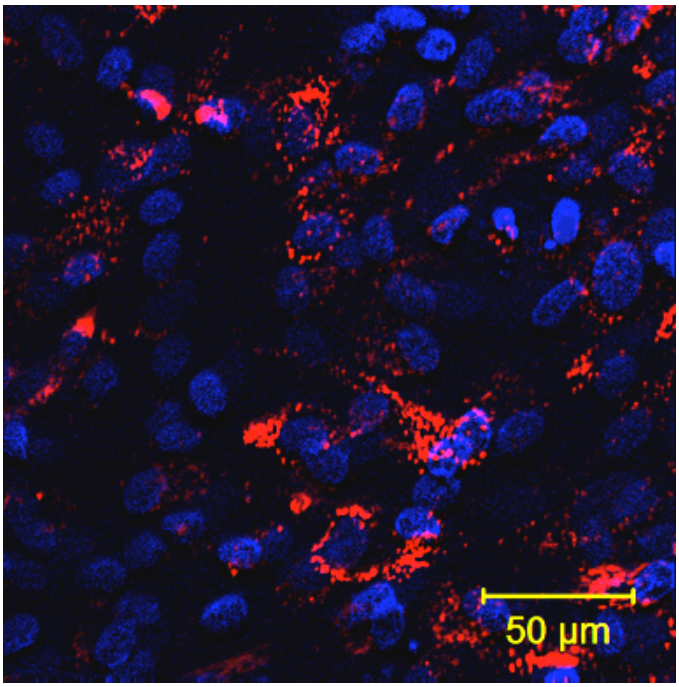

Fig. (4). A representative confocal photograph of a 10-day old culture of 625 nm Q-dot loaded ABMCs. The nuclei (blue) were stained with DAPI.

ABMCs was enhanced when the CM-DiI stock was prepared in DMSO rather than in ethanol and then diluted with HBSS to make the final working concentration that was added to the cells. After labeling, we found that CM-DiI could easily be detected in 87 ±4% (n = 8) of the ABMCs with the dye being primarily localized to the cell plasma membrane although some intracellular staining could be observed (Fig. **5**). In some cases, we observed that after labeling the ABMCs the CM-DiI fluorescence intensity would increase over several hours. This observation may possibly be due to the lipid solubility of CM-Dil and its movement within the cell where more of the molecule gets orientated in the correct position for maximal fluorescence emission [48]. Like the Q-dot labeled ABMCs, we found that after 10 days of culturing that the majority of the ABMCs (56 ± 0.02%, n =6) had retained the CM-Dil probe (Fig. **6**). However, for both Q-dots and CM-DiI there was a substantial loss of the probes by five weeks in culture that was likely due to a limiting dilution of the probes as a result of cell proliferation (unpublished observations).

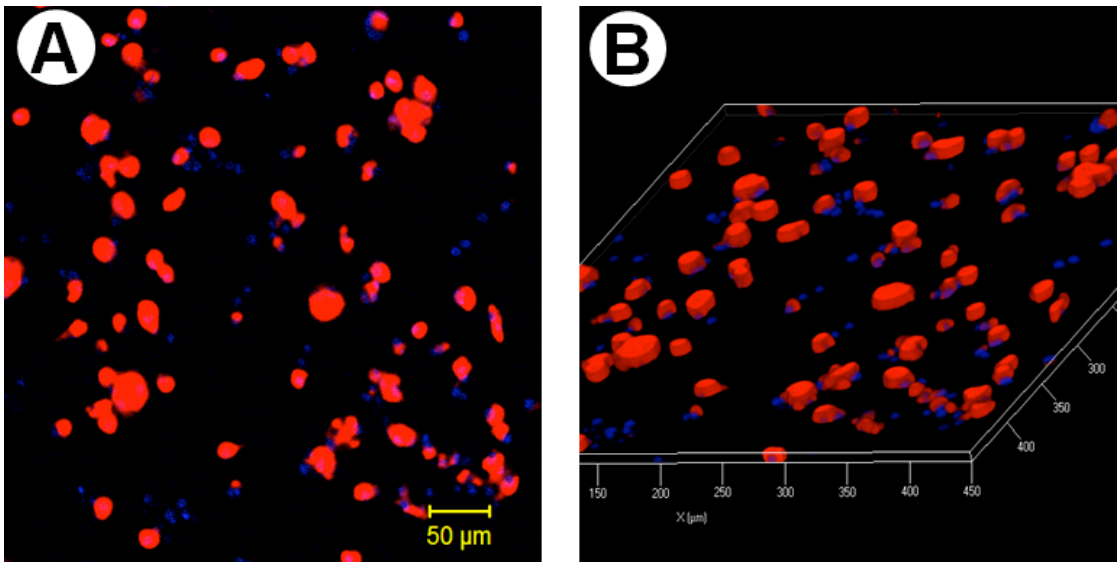

Fig. (5). CM-DiI labels the majority of porcine ABMCs. CM-DiI labeling was readily detectable in 78 ± 4% of ABMCs (n = 8). (**A**) A representative confocal photograph of CM-DiI labeled ABMCs 4-hrs after labeling. (**B**) A three dimensional reconstruction of Z-stack imaged cells showing the distribution of the CM-DiI within the ABMCs. The nuclei (blue) were stained with DAPI.

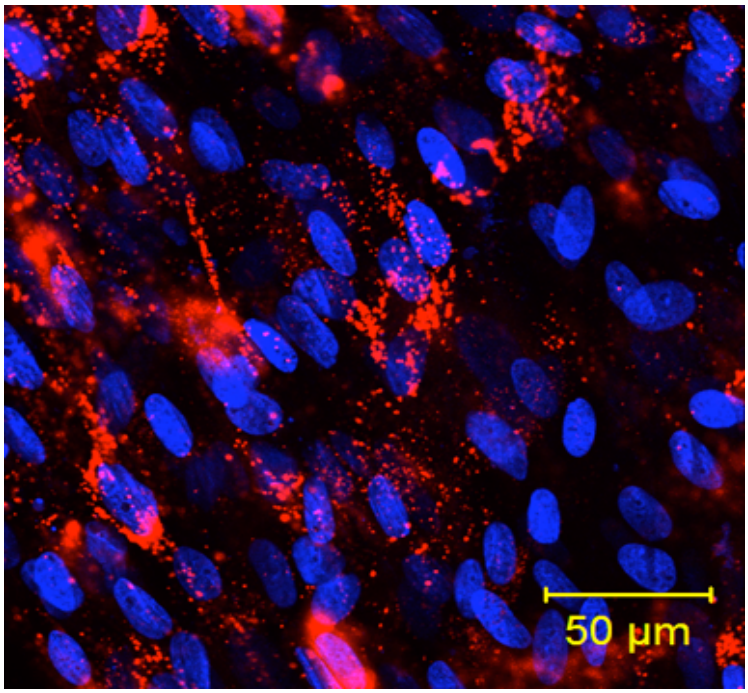

Fig. (6). A representative confocal photograph of a 10-day old culture of CM-Dil loaded ABMCs. The nuclei (blue) were stained with DAPI.

Effects of Labeled Bone Marrow on *In vitro* Assays

For any label used as a marker to track cells, it is important that it does not interfere with normal cell function. Studies have shown that the ability of the ABMCs to establish colony forming units (CFU-F) [14] and proliferate over time are important indicators of the therapeutic capacity of the ABMCs. We found that unlabeled ABMCs and CM-Dil or Q-dot labeled ABMCs on their ability to form *in vitro* colonies. Using an *in vitro* CFU-F assay we found that the labeling of ABMCs with CM-DiI had no significant ($p > 0.05$) effect on CFU-F formation compared to unlabeled cells (Fig. **7A**). In contrast the Q-dot labeled cells had a small but statistically significant ($p < 0.05$) effect on CFU-F formation (39 ±7; n=8) compared to unlabeled ABMCs (60.0 ±11; n=8) (Fig. **7B**).

In the next series of experiments, the Q-dot and CM-DiI probes were examined for their effects on ABMC proliferation using the MTT proliferation/cytotoxicity. The MTT growth assay has been used as a quantitative and convenient method for evaluating cellular growth or cytotoxicity effects in response to external or internal probes. In our study, we found that CM-DiI had no effect on ABMC proliferation when assessed at 7, 10 or 14 days following labeling (Fig. **8A**). In calculating the proliferation index (labeled and

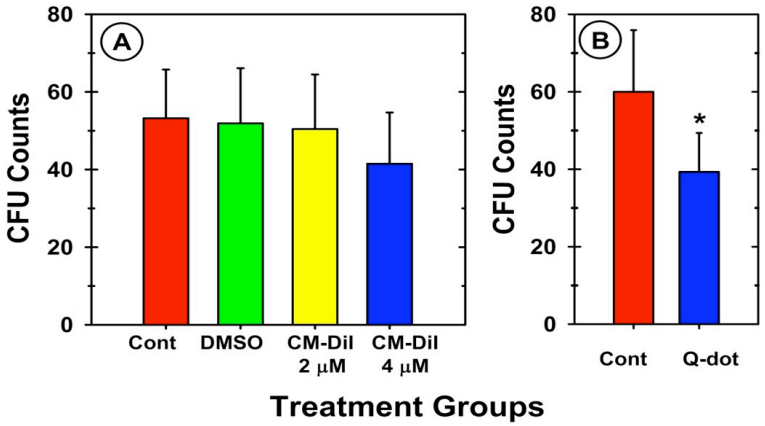

Fig. (7). CM-DiI and Q-dot labeling do not impair BMC CFU-F formation. Porcine ABMCs were labeled with (**A**) 2 μM or 4 μM CM-DiI or (**B**) 625nm Q-dots and analyzed 7 days later for CFU-F formation. Compared to unlabeled or DMSO-exposed BMC controls there was no significant effect ($p > 0.05$) of the CM-DiI (**7A**) on CFU-F formation but there was a small yet significant ($p < 0.05$) decrease (*) of the Q-dots on CFU-F formation (Fig. **7B**). Each point represents the mean ± SE of eight experiments.

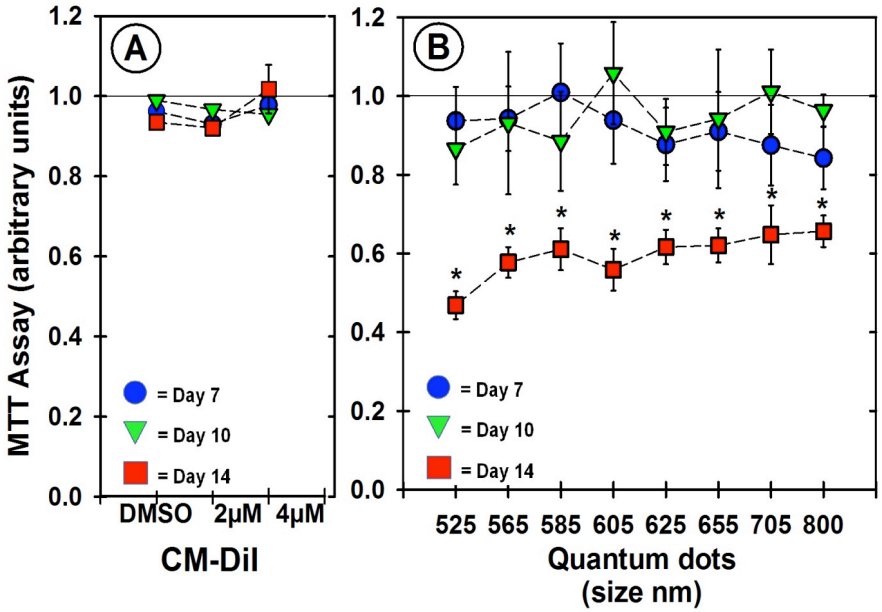

Fig. (8). Q-dot labeling, but not CM-DiI labeling, decreases long-term porcine BMC proliferation. ABMCs were labeled with either (**A**) CM-DiI or (**B**) Q-dots and then 7, 10, and 14 days later assayed for their level of proliferation compared to similarly cultured but unlabeled ABMCs. All values are expressed as the ratio of labeled/unlabeled ABMCs with a value of 1.0 representing no change in cell growth. Note that the DMSO control and 2μM or 4μM CM-DiI had no effect on cell proliferation at all time points (Fig. **8A**), but a significant ($p < 0.05$) decrease (*) in cell proliferation was observed by Q-dot labeled ABMCs at fourteen days of culture (Fig. **8B**). Each point represents the mean ± SE of six experiments.

unlabeled cells; PI) we found there was not a significant difference in the MTT optical density values between the CM-DiI labeled and unlabeled cells (Table **1**).

While labeling the ABMCs with Q-dots did not affect the ABMC proliferation measured 7 and 10 days later, we did find that the Q-dots did had a significant ($p < 0.05$) negative effect on ABMC proliferation at14 days (Fig. **8B**). This inhibitory effect of the Q-dots on ABMC proliferation was found for all sizes of the Q-dots used at 14 days (Fig. **8B**). This inhibitory effect of the Q-dots on cell growth can further be seen in Table **2** where there was a significant difference ($p < 0.05$) in the Proliferation Index between the Q-dot labeled and unlabeled cells at Day 14.

Live-Dead Cytotoxicity Assay of Freshly Labeled Q-dot ABMCs

Because of some partial negative effects of the Q-dots on *in vitro* cell function, we next wanted to examine whether the initial loading of the ABMCs with Q-dots would be compromising cell viability that may impact cell function.

Table 1. Data Showing the Proliferation Index (Ratio of DiI-Labeled to Unlabeled Cells) from the MTT Growth Assay Over a 14-Day Period (n = 6)

		DMSO	2 µM DiI	4 µM DiI
DAY 7	Proliferation Index	0.96	0.93	0.98
	±SE	±0.02	±0.03	±0.02
DAY 10	Proliferation Index	0.99	0.97	0.95
	±SE	±0.10	±0.01	±0.02
DAY 14	Proliferation Index	0.93	0.92	1.02
	±SE	±0.04	±0.03	±0.06

Table 2. Data Showing the Proliferation Index (Ratio of Q-Dot Labeled to Unlabeled Cells) from the MTT Growth Assay Over a 14-Day Period. Note that Compared to Day 7 and Day 10, a Significant Decrease (*; $p < 0.05$) was Observed in the Proliferation Index at Day 14 (n = 6)

		Qdot 525nm	Qdot 565nm	Qdot 585nm	Qdot 605nm	Qdot 625nm	Qdot 655nm	Qdot 705nm	Qdot 800nm
DAY 7	Proliferation Index	0.94	0.94	1.01	0.94	0.88	0.91	0.88	0.84
	±SE	±0.09	±0.08	±0.12	±0.11	±0.09	±0.10	±0.10	±0.08
DAY 10	Proliferation Index	0.87	0.93	0.89	1.06	0.91	0.94	1.01	0.96
	±SE	±0.09	±0.18	±0.13	±0.13	±0.08	±0.18	±0.11	±0.04
DAY 14	Proliferation Index	0.47	0.58	0.61	0.56	0.62	0.62	0.65	0.66
	±SE	±0.04*	±0.04*	±0.05*	±0.05*	±0.04*	±0.04*	±0.07*	±0.04*

Using a fluorescent Live-Dead cytotoxicity assay we found that there was no significant difference ($p > 0.05$) in the percentage of live viable cells between freshly unlabeled (96.49 ±0.48%; n=5) and Q-dot loaded ABMCs (98.34 ±0.33%; n=5) (Fig. **9**).

DISCUSSION

The use of bone marrow mononuclear progenitor cells for cell therapy is currently being investigated in a variety of clinical studies although questions still remain as to their mechanism of action [49]. One important aspect to help define the mechanism of ABMC action in tissue regeneration is to find a cell-tracking probe that can adequately label the cells without altering their cell function. The Q-dot nanocrystal and CM-DiI organic dye have both been used as cell trackers with varying success depending upon cell type [50]. In the current study, we evaluated the ability of Q-dots and CM-DiI to label adult porcine ABMCs and examined whether the labeling had any potential cytotoxic effects on the cells. We found that adult porcine ABMCs can be

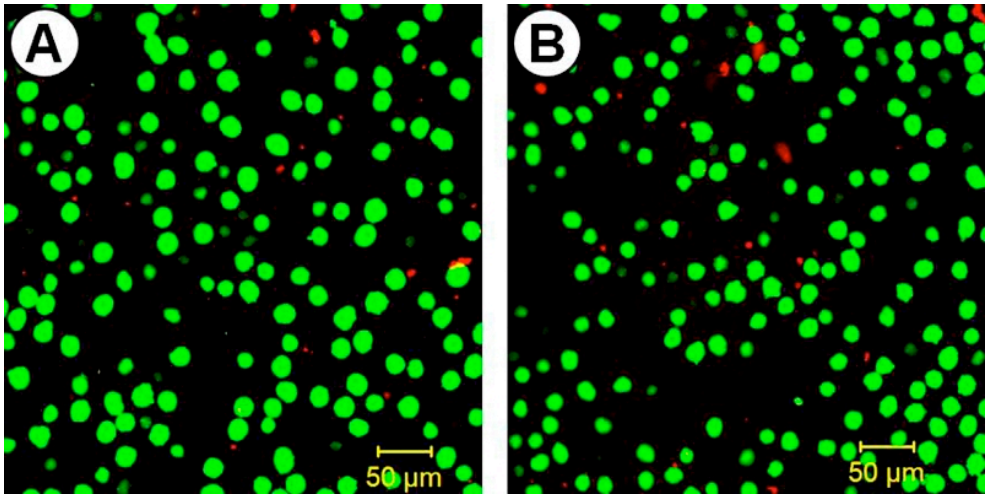

Fig. (9). Representative confocal images of the Live-Dead cytotoxicity stain on freshly isolated unlabeled ABMCs (Fig. **9A**) and 655 nm Q-dot labeled ABMCs (Fig. **9B**). The green (calcein-AM) represents viable cells whereas the red (ethidium bromide) represent dead cells.

labeled with either Q-dots or CM-DiI, that their migration and colony formation are not significantly impacted by either label, and that in regard to their proliferative capacity, Q-dot labeling, though not CM-DiI labeling, significantly inhibits ABMC proliferation.

Using modifications of the manufactures protocols we found the CM-DiI and Q-dot cell trackers could easily be loaded into porcine ABMCs. Because the Q-dots are now commercially available in a variety of sizes (Q-tracker kits, Molecular Probes/Invitrogen), we also felt it important to evaluate all of the different Q-dots sizes to determine if one was more effective than another for loading ABMCs. Following the manufacturer's instructions, we did find a variation in the relative loading effectiveness of the different sized Q-dots. That is, using the same labeling concentration of 10 nM for each of the Q-dot sizes we found that the 525 nm and 565 nm Q-dots were not as easily detected in ABMCs compared to the 585, 605, 625, 655, 705, and 800 nm Q-dots. Doubling the concentration of Q-dot binding peptide alone did not increase loading of the 525 nm and 565 nm Q-dots, but doubling both the binding peptide and Q-dot nanocrystal concentrations to 20 nM resulted in readily detectable loading of the 525 nm and 565 nm Q-dots within ABMCs. Similar to our porcine ABMC labeling results, it has been reported for human mesenchymal stem cells that the smaller 525 nm Q-dots did not load into cells as easily as the larger 655 nm Q-dots [51]. In our own study the reason for the easier loading of the ABMCs with Q-dots of sizes $\geq$585 nm is not entirely clear. It is known that translocation of Q-dots across cell membranes require a critical concentration of both the Q-dot nanocrystal and coating peptide [52, 53]. Although Q-dots are depicted in the literature as being spherical in shape, in reality Q-dots $\geq$585 nm are actually ellipsoid or rod-like in shape [54]. These Q-dot shape variations could result in differences in surface charge and therefore the amount of binding peptide allowing better uptake of the larger Q-dots [55]. The process of Q-dot uptake by cells appears to involve several different pathways including clathrin-mediated endocytosis [56], G-protein coupled mediated receptor uptake [57], or lipid-raft-dependent macropinocytosis [58]. However, the efficiency of these endocytic uptake mechanisms could also vary for different sized Q-dots. Despite Q-dot loading differences we did find that almost all of the ABMCs contained some Q-dot nanocrystals, but the actual number of Q-dots per cell was quite variable across the cell population. The variation in the amount of Q-dots within the ABMCs could be due to many factors including the heterogeneity of the bone marrow cell population itself.

We also found that a 2-4 μM solution of the organic dye CM-DiI could easily label the ABMCs and also within a shorter time period of 25 min compared to 70 min for complete loading of the cells with the Q-dots. If a time critical experiment exists where the stem cells need to be injected back into the animal as soon as possible, then loading the cells with CM-DiI has clear advantages over Q-dots. Unlike the Q-dots, which were always found within the cell cytoplasm, the overall localization of CM-DiI within the ABMCs was limited to the plasma membrane with some intracellular staining. The CM-DiI fluorescence we observed within ABMCs has also been reported for other cell types and is consistent with the lipophilic structure of CM-DiI [59].

In addition to labeling cells, Q-dots and CM-DiI were assessed for their impact on cell function. We found that loading the ABMCs with CM-DiI had no effect of the ABMCs to form colonies in a CFU-F assay, but that Q-dot labeled ABMCs had a small but significant inhibitory effect on CFU-F formation. We also found that clear differences between the Q-dot and CM-DiI probes in their long-term impact on cell proliferation. Compared to controls there was no difference between Q-dot and CM-DiI labeled ABMCs at 7 and 10 days, but after two weeks in culture the Q-dot loaded ABMCs had significantly lower growth rates as compared to unlabeled ABMCs. This reduction in ABMC growth was detectable with all the Q-dot sizes used, suggesting that the underlying toxic effect may be independent of Q-dot size. This Q-dot cytotoxic effect on the ABMCs at a later time was not due to the immediate consequence of loading the cells with the Q-dots since we found no change in ABMC cell viability using a Live-Dead cytotoxicity assay. Other studies looking at Q-dot toxicity on cells have reported varying results, which could be attributed to the different types of Q-dots used, their core shell thicknesses, and the cell type used for labeling [36, 60]. Although not examined in our study, others have shown that Q-dots can have some cytotoxic effects on cells by the upregulation of the Fas receptor and lipid peroxidation [61].

Although we did not find CM-DiI to alter ABMC cell proliferation, it should be noted that this probe is not without its potential problems or toxic effects on cells. In preliminary experiments we observed that CM-DiI $\geq$ 6 μM reduced BMC viability. The tolerance of cells to CM-DiI is quite variable with labeling solutions of CM-DiI $\geq$ 6μM having been reported to impair sheep mesenchymal cell division [33], but a labeling solution of 20 μM CM-DiI had no reported effect on human bone marrow fibroblast viability [62]. It should also be noted that although the transfer of CM-DiI to other cells has not been detected [63], others have reported CM-Dil transfer to other cells after injection into the animal [50, 64]. As mentioned by Kruyt and colleagues [65], that transfer of CM-Dil from labeled dead cells or via direct membrane contact cannot be ruled out in any study. However, if used at the correct doses, studies have shown that CM-DiI labeled cells can be detected within tissues from three to eight weeks after injection into the animal [1, 33, 37]. Of interest is the fact that CM-DiI was easily retained within sheep mesenchymal stem cells for six weeks whereas carboxy-fluorescein diacetate succinimidyl ester (CFSE) showed a rapid loss in these same cells just eight days after loading [33]. These data suggest that the use and retention of any organic fluorescent probe is likely to be specific to each individual cell type.

The fact that the CM-DiI probe is well retained in cells throughout standard formalin tissue fixation gives it an advantage over Q-dot labeled cells due to the fact that small concentrations of paraformaldehyde or methanol fixative can alter Q-dot fluorescence in cells [39]. However, even the best organic dye or Q-dot labeled cell will be difficult to track in tissues due to a limiting dilution of the cell probe as a result from cell division [66]. It is also important to note that

nanoparticles like Q-dots can also be eliminated from cells not only by cell division but also by an autophagic flux from the cells [67]. In loading human mesenchymal stem cells with Q-tracker kits of Q-dot 525 nm and Q-dot 605 nm it was observed that there was an asymmetric retention of these two trackers that the Q-dot 525 was almost entirely eliminated after three to four days in culture whereas the Q-dot 605 could still easily be observed [45, 67].

In the case of labeling ABMCs with Q-dots our results suggest that the optimal timeframe for using Q-dots to track labeled ABMCs within an animal would be within the first 10 days after labeling where toxicity to the cells is at a minimum. Future studies of tracking ABMCs long-term will likely require the use of both short-term and long-term cell labels, with long-term cell labels possibly involving stable gene transfection of fluorescent proteins [68, 69].

CONCLUSION

Our study found that the cell trackers Q-dots or CM-DiI could effectively label porcine ABMCs. However, because bone marrow does contains multiple cell types such as hematopoietic progenitor cells, stromal stem cells, monocytes, and other stem cells, it is unknown at this time how efficiently the Q-dots or CM-DiI can label each of these cell types. In addition, both Q-dot and CM-DiI labeled cells could also be detected after two weeks in cell culture, but we do not yet know the identity of these cultured cells and it is very likely that they also contain a mixed population of cells. We also found differences with the Q-dots and CM-DiI on *in vitro* ABMC function. That is, CM-DiI labeled ABMCs had no significant impact on either CFU-F or cell proliferation. However, the Q-dot labeled ABMCs had a small but significant inhibitory effect on CFU-F formation as well as inhibition of cell proliferation at two weeks. In this regard, it could be possible that the proportions of the various bone marrow cell types from isolation to isolation could also account for some of the variation in the outcome of different experiments. Overall, our results suggest that for long-term tracking studies that the organic CM-DiI fluorescent probe will be more useful than Q-dots for labeling porcine ABMCs. Work is currently in progress to isolate and define the different cell types within porcine bone marrow for a better understanding of their responses to cell labeling, function, and culture conditions.

ACKNOWLEDGEMENTS

We would like to thank Rebecca Sarao, Ping-Cheng Wu, and Jeffrey Teach for the collection of the bone marrow samples, and Lian Wang and Ann Romer for assistance with the SEPAX bone marrow processing. We would also like to thank Dr. Greg Cox (Molecular MD) for his advice in the early parts of this study and Dr. Iain Johnson (Molecular Probes) for his helpful suggestions and samples of Q-dots. This study was funded in part by the Department of the Army Grant #W81XWH-05-1-0586 and in part by the Armed Forces Institute of Regenerative Medicine (AFIRM) #W81XWH-08-2-0032. The content of the information does not necessarily reflect the position of the Federal Government and no official endorsement should be inferred.

REFERENCES

[1] Makela J, Ylitalo K, Lehtonen S, *et al*. Bone marrow-derived mononuclear cell transplantation improves myocardial recovery by enhancing cellular recruitment and differentiation at the infarction site. J Thorac Cardiovasc Surg 2007; 134: 565-73.

[2] Ly HQ, Hoshino K, Pomerantseva I, *et al*. *In vivo* myocardial distribution of multipotent progenitor cells following intracoronary delivery in a swine model of myocardial infarction. Eur Heart J 2009; 30: 2861-8.

[3] Sheu JJ, Yuen CM, Sun CK, *et al*. Six-month angiographic study of immediate autologous bone marrow mononuclear cell implantation on acute anterior wall myocardial infarction using a mini-pig model. Int Heart J 2009; 50: 221-34.

[4] Graham JJ, Foltz WD, Vaags AK, *et al*. Long-term tracking of bone marrow progenitor cells following intracoronary injection post-myocardial infarction in swine using MRI. Am J Physiol Heart Circ Physiol 2010; 299: H125-33.

[5] Kale S, Karihaloo A, Clark PR, Kashgarian M, Krause DS, Cantley LG. Bone marrow stem cells contribute to repair of the ischemically injured renal tubule. J Clin Invest 2003; 112: 42-9.

[6] Poulsom R, Alison MR, Cook T, *et al*. Bone marrow stem cells contribute to healing of the kidney. J Am Soc Nephrol 2003; 14(Suppl 1): S48-54.

[7] Jung YJ, Ryu KH, Cho SJ, *et al*. Syngenic bone marrow cells restore hepatic function in carbon tetrachloride-induced mouse liver injury. Stem Cells Dev 2006; 15: 687-95.

[8] Akiyama Y, Radtke C, Honmou O, Kocsis JD. Remyelination of the spinal cord following intravenous delivery of bone marrow cells. Glia 2002; 39: 229-36.

[9] Shimizu S, Kitada M, Ishikawa H, Itokazu Y, Wakao S, Dezawa M. Peripheral nerve regeneration by the *in vitro* differentiated-human bone marrow stromal cells with Schwann cell property. Biochem Biophys Res Commun 2007; 359: 915-20.

[10] Zhang P, He X, Liu K, *et al*. Bone marrow stromal cells differentiated into functional Schwann cells in injured rats sciatic nerve. Artif Cells Blood Substit Immobil Biotechnol 2004; 32: 509-18.

[11] Cuevas P, Carceller F, Dujovny M, *et al*. Peripheral nerve regeneration by bone marrow stromal cells. Neurol Res 2002; 24: 634-8.

[12] van der Bogt KE, Sheikh AY, Schrepfer S, *et al*. Comparison of different adult stem cell types for treatment of myocardial ischemia. Circulation 2008; 118: S121-9.

[13] Assmus B, Rolf A, Erbs S, Elsasser A, *et al*. Clinical outcome 2 years after intracoronary administration of bone marrow-derived progenitor cells in acute myocardial infarction. Circ Heart Fail 2010; 3: 89-96.

[14] Assmus B, Fischer-Rasokat U, Honold J, *et al*. Transcoronary transplantation of functionally competent BMCs is associated with a decrease in natriuretic peptide serum levels and improved survival of patients with chronic postinfarction heart failure: results of the TOPCARE-CHD Registry. Circ Res 2007; 100: 1234-41.

[15] Assmus B, Honold J, Schachinger V, Britten MB, *et al*. Transcoronary transplantation of progenitor cells after myocardial infarction. N Engl J Med 2006; 355: 1222-32.

[16] Erbs S, Linke A, Schachinger V, *et al*. Restoration of microvascular function in the infarct-related artery by intracoronary transplantation of bone marrow progenitor cells in patients with acute myocardial infarction: the Doppler Substudy of the Reinfusion of Enriched Progenitor Cells and Infarct Remodeling in Acute Myocardial Infarction (REPAIR-AMI) trial. Circulation 2007; 116: 366-74.

[17] Gee AP, Richman S, Durett A, *et al*. Multicenter cell processing for cardiovascular regenerative medicine applications: the Cardiovascular Cell Therapy Research Network (CCTRN) experience. Cytotherapy 2010; 12: 648-91.

[18] Matoba S, Tatsumi T, Murohara T, *et al*. Long-term clinical outcome after intramuscular implantation of bone marrow mononuclear cells (Therapeutic Angiogenesis by Cell Transplantation [TACT] trial) in patients with chronic limb ischemia. Am Heart J 2008; 156: 1010-8.

[19] Cobellis G, Silvestroni A, Lillo S, *et al*. Long-term effects of repeated autologous transplantation of bone marrow cells in patients affected by peripheral arterial disease. Bone Marrow Transplant 2008; 42: 667-72.

[20] Amann B, Ludemann C, Ruckert R, *et al*. Design and rationale of a randomized, double-blind, placebo-controlled phase III study for autologous bone marrow cell transplantation in critical limb ischemia: the BONe Marrow Outcomes Trial in Critical Limb Ischemia (BONMOT-CLI). Vasa 2008; 37: 319-25.

[21] Bartsch T, Brehm M, Zeus T, Kogler G, Wernet P, Strauer BE. Transplantation of autologous mononuclear bone marrow stem cells in patients with peripheral arterial disease (the TAM-PAD study). Clin Res Cardiol 2007; 96: 891-9.

[22] Nizankowski R, Petriczek T, Skotnicki A, Szczeklik A. The treatment of advanced chronic lower limb ischaemia with marrow stem cell autotransplantation. Kardiol Pol 2005; 63: 351-60; discussion 61.

[23] Sussman MA, Murry CE. Bones of contention: marrow-derived cells in myocardial regeneration. J Mol Cell Cardiol 2008; 44: 950-3.

[24] Hosoda T, Kajstura J, Leri A, Anversa P. Mechanisms of myocardial regeneration. Circ J 2010; 74: 13-7.

[25] Brenneman M, Sharma S, Harting M, *et al*. Autologous bone marrow mononuclear cells enhance recovery after acute ischemic stroke in young and middle-aged rats. J Cereb Blood Flow Metab 2010; 30(1): 140-9.

[26] Burchfield JS, Dimmeler S. Role of paracrine factors in stem and progenitor cell mediated cardiac repair and tissue fibrosis. Fibrogen Tissue Repair 2008; 1: 4.

[27] Rota M, Kajstura J, Hosoda T, *et al*. Bone marrow cells adopt the cardiomyogenic fate *in vivo*. Proc Natl Acad Sci USA 2007; 104: 17783-8.

[28] Hofmann M, Wollert KC, Meyer GP, *et al*. Monitoring of bone marrow cell homing into the infarcted human myocardium. Circulation 2005; 111: 2198-202.

[29] Zhou R, Acton PD, Ferrari VA. Imaging stem cells implanted in infarcted myocardium. J Am Coll Cardiol 2006; 48: 2094-106.

[30] Nyolczas N, Charwat S, Posa A, *et al*. Tracking the migration of cardially delivered therapeutic stem cells *in vivo*: state of the art. Regen Med 2009; 4: 407-22.

[31] van der Spoel TI, Lee JC, Vrijsen K, *et al*. Non-surgical stem cell delivery strategies and *in vivo* cell tracking to injured myocardium. Int J Cardiovasc Imaging 2010; [Epub ahead of print].

[32] Li Z, Lee A, Huang M, Chun H, *et al*. Imaging survival and function of transplanted cardiac resident stem cells. J Am Coll Cardiol 2009; 53: 1229-40.

[33] Weir C, Morel-Kopp MC, Gill A, *et al*. Mesenchymal stem cells: isolation, characterisation and *in vivo* fluorescent dye tracking. Heart Lung Circ 2008; 17: 395-403.

[34] Stoff A, Rivera AA, Sanjib Banerjee N, *et al*. Promotion of incisional wound repair by human mesenchymal stem cell transplantation. Exp Dermatol 2009; 18: 362-9.

[35] Jaiswal JK, Goldman ER, Mattoussi H, Simon SM. Use of quantum dots for live cell imaging. Nat Methods 2004; 1: 73-8.

[36] Jaiswal JK, Simon SM. Optical monitoring of single cells using quantum dots. Methods Mol Biol 2007; 374: 93-104.

[37] Ruhparwar A, Kofidis T, Ruebesamen N, Karck M, Haverich A, Martin U. Intra-vital fluorescence microscopy for intra-myocardial graft detection following cell transplantation. Int J Cardiovasc Imaging 2005; 21: 569-74.

[38] Dai W, Hale SL, Martin BJ, *et al*. Allogeneic mesenchymal stem cell transplantation in postinfarcted rat myocardium: short- and long-term effects. Circulation 2005; 112: 214-23.

[39] Williams Y, Byrne S, Bashir M, *et al*. Comparison of three cell fixation methods for high content analysis assays utilizing quantum dots. J Microsc 2008 ; 232: 91-8.

[40] Deerinck TJ. The application of fluorescent quantum dots to confocal, multiphoton, and electron microscopic imaging. Toxicol Pathol 2008; 36: 112-6.

[41] Gao X, Chan WC, Nie S. Quantum-dot nanocrystals for ultrasensitive biological labeling and multicolor optical encoding. J Biomed Opt 2002; 7: 532-7.

[42] Jaiswal JK, Mattoussi H, Mauro JM, Simon SM. Long-term multiple color imaging of live cells using quantum dot bioconjugates. Nat Biotechnol 2003; 21: 47-51.

[43] Lin S, Xie X, Patel MR, *et al*. Quantum dot imaging for embryonic stem cells. BMC Biotechnol 2007; 7: 67.

[44] Dupont KM, Sharma K, Stevens HY, Boerckel JD, Garcia AJ, Guldberg RE. Human stem cell delivery for treatment of large segmental bone defects. Proc Natl Acad Sci USA 2010; 107: 3305-10.

[45] Seleverstov O, Phang JM, Zabirnyk O. Semiconductor nanocrystals in autophagy research: methodology improvement at nanosized scale. Methods Enzymol 2009; 452: 277-96.

[46] Aktas M, Radke TF, Strauer BE, Wernet P, Kogler G. Separation of adult bone marrow mononuclear cells using the automated closed separation system Sepax. Cytotherapy 2008; 10: 203-11.

[47] Zinkl JG, Jain N. Schalm's Veterinary Hematology. 5th ed. Philadelphia, Pennsylvania: Lippincott Williams & Wilkins 2000.

[48] Axelrod D. Carbocyanine dye orientation in red cell membrane studied by microscopic fluorescence polarization. Biophys J 1979; 26: 557-73.

[49] Aicher A, Heeschen C, Feil S, *et al*. cGMP-dependent protein kinase I is crucial for angiogenesis and postnatal vasculogenesis. PLoS One 2009; 4: e4879.

[50] Schormann W, Hammersen FJ, Brulport M, *et al*. Tracking of human cells in mice. Histochem Cell Biol 2008; 130: 329-38.

[51] Rosen AB, Kelly DJ, Schuldt AJ, *et al*. Finding fluorescent needles in the cardiac haystack: tracking human mesenchymal stem cells labeled with quantum dots for quantitative *in vivo* three-dimensional fluorescence analysis. Stem Cells 2007; 25: 2128-38.

[52] Medintz IL, Pons T, Delehanty JB, *et al*. Intracellular delivery of quantum dot-protein cargos mediated by cell penetrating peptides. Bioconjug Chem 2008; 19: 1785-95.

[53] Mattheakis LC, Dias JM, Choi YJ, *et al*. Optical coding of mammalian cells using semiconductor quantum dots. Anal Biochem 2004; 327: 200-8.

[54] Giepmans BN, Deerinck TJ, Smarr BL, Jones YZ, Ellisman MH. Correlated light and electron microscopic imaging of multiple endogenous proteins using Quantum dots. Nat Methods 2005; 2: 743-9.

[55] Wei Y, Jana NR, Tan SJ, Ying JY. Surface Coating Directed Cellular Delivery of TAT-Functionalized Quantum Dots. Bioconjug Chem 2009; 20: 1752-8.

[56] Anas A, Okuda T, Kawashima N, *et al*. Clathrin-mediated endocytosis of quantum dot-peptide conjugates in living cells. ACS Nano 2009; 3: 2419-29.

[57] Zhang LW, Monteiro-Riviere NA. Mechanisms of quantum dot nanoparticle cellular uptake. Toxicol Sci 2009; 110: 138-55.

[58] Chen B, Liu Q, Zhang Y, Xu L, Fang X. Transmembrane delivery of the cell-penetrating peptide conjugated semiconductor quantum dots. Langmuir 2008; 24: 11866-71.

[59] Honig MG, Hume RI. Fluorescent carbocyanine dyes allow living neurons of identified origin to be studied in long-term cultures. J Cell Biol 1986; 103: 171-87.

[60] Pelley JL, Daar AS, Saner MA. State of academic knowledge on toxicity and biological fate of quantum dots. Toxicol Sci 2009; 112: 276-96.

[61] Choi AO, Cho SJ, Desbarats J, Lovric J, Maysinger D. Quantum dot-induced cell death involves Fas upregulation and lipid peroxidation in human neuroblastoma cells. J Nanobiotechnol 2007; 5: 1.

[62] Ferrari A, Hannouche D, Oudina K, *et al*. *In vivo* tracking of bone marrow fibroblasts with fluorescent carbocyanine dye. J Biomed Mater Res 2001; 56: 361-7.

[63] Andrade W, Seabrook TJ, Johnston MG, Hay JB. The use of the lipophilic fluorochrome CM-DiI for tracking the migration of lymphocytes. J Immunol Methods 1996; 194: 181-9.

[64] Brulport M, Schormann W, Bauer A, *et al*. Fate of extrahepatic human stem and precursor cells after transplantation into mouse livers. Hepatology 2007; 46: 861-70.

[65] Kruyt MC, De Bruijn J, Veenhof M, *et al*. Application and limitations of chloromethyl-benzamidodialkylcarbocyanine for tracing cells used in bone Tissue engineering. Tissue Eng 2003; 9: 105-15.

[66] Lyons AB. Divided we stand: tracking cell proliferation with carboxyfluorescein diacetate succinimidyl ester. Immunol Cell Biol 1999; 77: 509-15.

[67] Seleverstov O, Zabirnyk O, Zscharnack M, *et al*. Quantum dots for human mesenchymal stem cells labeling. A size-dependent autophagy activation. Nano Lett 2006; 6: 2826-32.

[68] Li SH, Lai TY, Sun Z, *et al*. Tracking cardiac engraftment and distribution of implanted bone marrow cells: Comparing intra-

aortic, intravenous, and intramyocardial delivery. J Thorac Cardiovasc Surg 2009; 137: 1225-33 e1.

[69] Weber K, Bartsch U, Stocking C, Fehse B. A multicolor panel of novel lentiviral "gene ontology" (LeGO) vectors for functional gene analysis. Mol Ther 2008; 16: 698-706.

Received: May 12, 2010 Revised: October 04, 2010 Accepted: October 22, 2010